



Substantial contribution of tree canopy nitrifiers to nitrogen fluxes in European forests

Received: 11 July 2022

Accepted: 14 December 2023

Published online: 8 February 2024

Check for updates

Rossella Guerrieri ^{1,2}, Joan Cáliz ³, Stefania Mattana ^{2,4}, Anna Barceló ⁵, Marco Candela ⁶, David Elustondo ⁷, Heike Fortmann ⁸, Sofie Hellsten ⁹, Nils Koenig ⁸, Antti-Jussi Lindroos ¹⁰, Giorgio Matteucci ¹¹, Päivi Merilä ¹⁰, Greg Michalski ¹², Manuel Nicolas ¹³, Anne Thimonier ¹⁴, Silvia Turroni ⁶, Elena Vanguelova ¹⁵, Arne Verstraeten ¹⁶, Peter Waldner ¹⁴, Mirai Watanabe ¹⁷, Emilio O. Casamayor ³, Josep Peñuelas ^{2,4} & Maurizio Mencuccini ^{2,18}

Human activities have greatly increased the reactive nitrogen in the biosphere, thus profoundly altering global nitrogen cycling. The large increase in nitrogen deposition over the past few decades has led to eutrophication in natural ecosystems, with negative effects on forest health and biodiversity. Recent studies, however, have reported oligotrophication in forest ecosystems, constraining their capacity as carbon sinks. Here we demonstrate the widespread biological transformation of atmospheric reactive nitrogen in the canopies of European forests by combining nitrogen deposition quantification with measurements of the stable isotopes in nitrate and molecular analyses across ten forests through August–October 2016. We estimate that up to 80% of the nitrate reaching the soil via throughfall was derived from canopy nitrification, equivalent to a flux of up to $5.76 \text{ kg N ha}^{-1} \text{ yr}^{-1}$. We also document the presence of autotrophic nitrifiers on foliar surfaces throughout European forests. Canopy nitrification thus consumes deposited ammonium and increases nitrate inputs to the soil. The results of this study highlight widespread canopy nitrification in European forests and its important contribution to forest nitrogen cycling.

Nitrogen is one of the main elements on Earth. It links the atmosphere with terrestrial and aquatic ecosystems via biogeochemical processes. Reactive nitrogen in the atmosphere has doubled over the last century as a result of the combustion of fossil fuels and the intensive use of fertilizers in food production to sustain global population growth¹, extending planetary boundaries for nitrogen fluxes beyond a safe limit². Elevated rates of nitrogen deposition are one of the drivers of the increased strength of forest carbon sinks^{3,4}, particularly in

nitrogen-limited ecosystems in temperate and boreal biomes, thus contributing to the mitigation of climate change. The global increase in nitrogen deposition, however, generates cascading effects and contributes to the acceleration of nitrogen cycling⁵, which has important implications for both natural ecosystems functioning and human health^{6–8}. Tracing and quantifying the fate of atmospheric nitrogen when moving from the atmosphere to the soil through forest canopies is paramount to quantifying its effects on terrestrial carbon and nitrogen

A full list of affiliations appears at the end of the paper. e-mail: r.guerrieri@unibo.it

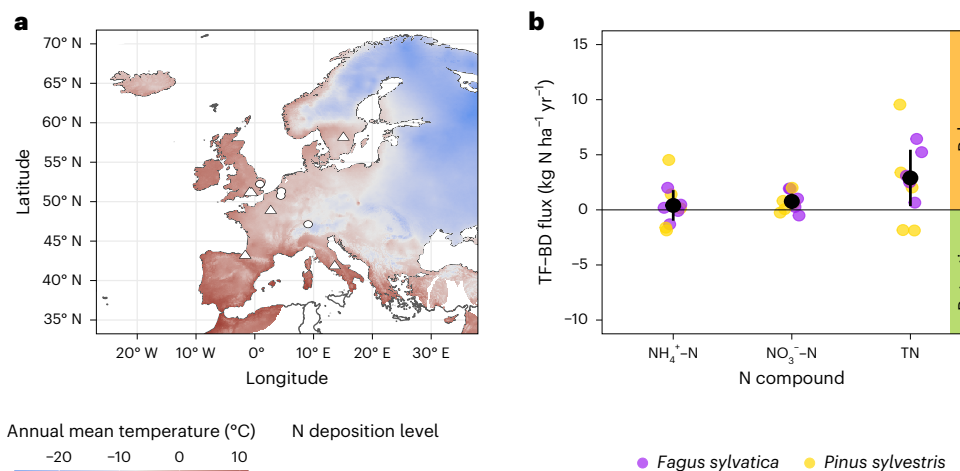


Fig. 1 | Investigated sites and wet deposition fluxes of inorganic nitrogen. **a**, Map showing the forested sites included in this study. **b**, Difference between TF and BD for the nitrogen fluxes $\text{NH}_4^+ \text{-N}$, $\text{NO}_3^- \text{-N}$ and TN. Means and 95% confidence intervals for nitrogen forms across the sites are indicated in black ($n = 10$, data are reported in Extended Data Table 2). Orange and green rectangles

to the right indicate, respectively, the range of apparent release (source) and apparent retention (sink) of nitrogen compounds by forest canopies. The daily updated E-OBS dataset for temperature (1950–2021) from the Copernicus Climate Change Service was used to produce the map (https://surfobs.climate.copernicus.eu/dataaccess/access_eobs.php).

cycling. This is particularly important for nitrogen in the form of nitrate (NO_3^-), a highly mobile compound that can be readily lost by leaching and denitrification when its availability exceeds plant and microbial demands⁹. Nitrate concentration in soil solutions is a key indicator of nitrogen saturation in forest ecosystems⁹, setting the threshold for the critical nitrogen loads (CLs) beyond which ecosystem processes and plant community compositions can shift^{10–12}. Indeed, the seminal hypothesis of nitrogen saturation⁹ suggests that nitrogen deposition accumulates in soil nitrogen pools and progressively increases mineralization and nitrification, eventually leading to an excess of nitrogen availability compared to the demand from plants, as well as to elevated NO_3^- leaching and the emission of trace gases (particularly N_2O). Negative effects of nitrogen saturation on soil processes and tree health have been reported in soil manipulation studies^{13,14}, often following the application of nitrogen doses much higher than ambient nitrogen deposition, thus exposing ecosystems to larger changes in atmospheric nitrogen input than those projected in all scenarios of the IPCC Representative Concentration Pathway¹⁵. Field studies across Europe and North America have confirmed an increase in NO_3^- leaching at sites exceeding nitrogen depositions of $10 \text{ kg ha}^{-1} \text{ yr}^{-1}$, but there is no clear evidence that this pathway of nitrogen loss (and hence saturation) increases over time under increasing nitrogen deposition¹⁶. In contrast, recent analyses have identified pervasive nitrogen limitations in forests ('too little of a good thing' or oligotrophication)^{17,18}, which can constrain the expected CO_2 fertilization effect^{19–21}.

Atmospheric nitrogen undergoes complex transformations in its trajectory from the atmosphere to the soil, including interactions with forest canopies and the associated microbial communities^{22,23}. Evidence since the 1980s has shown that fluxes in precipitation are substantially affected when passing through forest canopies²³. These studies have led to the quantification of fluxes underneath tree canopies (so-called throughfall, TF) to better estimate the total input of nitrogen from atmospheric deposition (including dry reactive nitrogen compounds) and the proportion eventually reaching the soil. The differences between TF and open-field deposition (either wet deposition or, as in our study, bulk deposition, BD) of nitrogen in the form of ammonium ($\text{NH}_4^+ \text{-N}$) and $\text{NO}_3^- \text{-N}$ have been extensively used to determine whether tree canopies act as sinks (TF – BD < 0, canopy retention) or sources (TF – BD > 0, canopy release) of nitrogen compounds (including deposited dry compounds^{24–26}, as well as ionic exchanges between

canopies and aqueous solutions)^{27,28}. Investigations of canopy nitrogen retention or release have mostly focused on the passive role of foliar surfaces to retain nitrogen compounds from the atmosphere (particularly the dry forms), which affects the input of these compounds to the soil. However, next-generation sequencing analyses have begun to unravel the highly diverse microbial communities living in forest canopies^{29,30} and to identify, *in situ*, the taxa contributing to processes that were previously considered to occur only in soil^{31,32}. Previous studies have found that nitrate in TF water represents not only a flux from atmospheric deposition, but also from biological nitrification in tree canopies^{33–34}. Whether microbes transform nitrogen in forest canopies across a wide range of forest types, climatic conditions and levels of atmospheric deposition, and how they contribute to NO_3^- fluxes reaching the soil via TF, have not yet been determined. In this Article we examine the importance of microbially driven canopy nitrification in the context of the ongoing debate surrounding the trajectories of apparent ecosystem nitrogen saturation and tree oligotrophication. We combine isotopic and genetic analyses to estimate canopy nitrification across European forests, to identify microorganisms potentially involved in this process, and to quantify the contribution of gross canopy nitrification (GCN) to nitrogen fluxes. Ten sites included in the European International Co-operative Programme on Assessment and Monitoring of Air Pollution Effects on Forests (ICP Forests) were chosen that include the two most dominant tree species in Europe (*Fagus sylvatica* L. and *Pinus sylvestris* L., hereafter *F. sylvatica* and *P. sylvestris*, respectively). Forests were selected along wide gradients of climate and wet deposition of inorganic nitrogen (Fig. 1 and Extended Data Table 1), with levels of nitrogen deposition below and above the empirical CLs of $10–15 \text{ kg ha}^{-1} \text{ yr}^{-1}$ (ref. 35). We consider fluxes of BD and TF nitrogen deposition measured in 2016 across the investigated sites to determine whether tree canopies act as apparent sinks (retention) or apparent sources (release) of atmospheric reactive nitrogen compounds, focusing on $\text{NH}_4^+ \text{-N}$, $\text{NO}_3^- \text{-N}$ and total nitrogen (TN, including dissolved organic nitrogen). We use isotopic tracers, particularly $\Delta^{17}\text{O}$ (defined as $\Delta^{17}\text{O} = \delta^{17}\text{O} - 0.52 \times \delta^{18}\text{O}$) in NO_3^- , in a two-end-member isotope model, to estimate the atmospheric (f_{Atm}) and biological (f_{Bio}) fractions contributing to NO_3^- recovered in TF water. $\Delta^{17}\text{O}$ is a robust tool for quantifying the contributions of the two sources of NO_3^- directly reaching the TF (atmospheric deposition and canopy nitrification), due to the distinctive $\Delta^{17}\text{O}$ values of

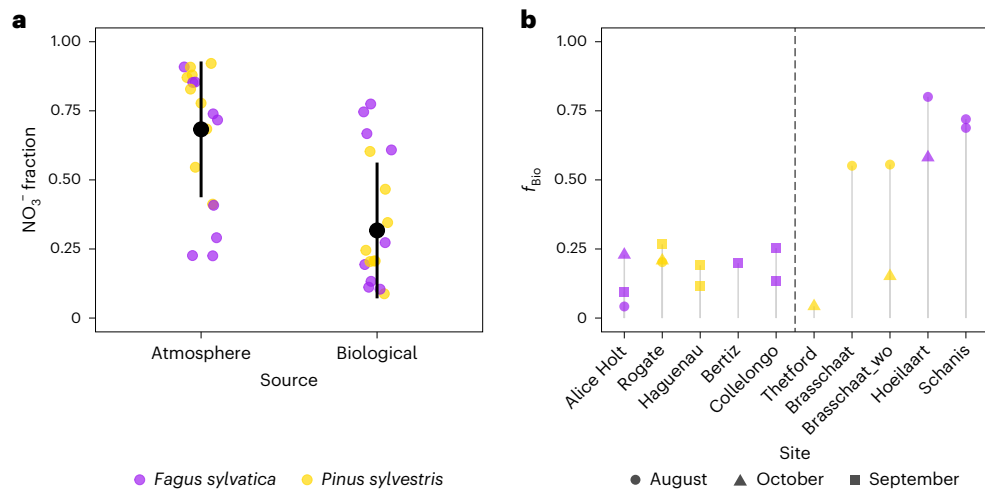


Fig. 2 | Atmopsherically and biologically derived nitrate fractions. **a**, Fraction of NO_3^- derived from atmospheric deposition and biological nitrification in tree canopies for the two species across the investigated sites. Means and s.d. values are shown in black. **b**, Fraction of NO_3^- from canopy nitrification (f_{Bio}) measured at each site for each sampling date. The calculation of f_{Bio} for Brasschaat in Belgium was obtained from $\Delta^{17}\text{O}$ in NO_3^- collected in BD and wet-only precipitation (wo)

collectors (see Methods for more details). The Swedish site was not included in the isotope analyses, because canopy retention was observed but no canopy nitrification was detected (Extended Data Fig. 1 and Extended Data Tables 2 and 4). The dashed vertical grey line in **b** separates sites with low (left) and high (right) nitrogen deposition, identified as explained in the main text and Methods.

the two sources (positive values for atmospheric NO_3^- and a value of zero for microbial NO_3^-)³⁶ (Methods). Finally, we document the presence in the canopy of microorganisms and key bacterial and archaeal genes that drive nitrification, using 16S rRNA gene metabarcoding and gene-specific quantitative polymerase chain reaction (qPCR) for genes that encode for ammonia monooxygenase subunit A (*amoA*) and nitrite oxidoreductase subunit B (*nxrB*), catalysing the oxidation of ammonia to nitrite and of nitrite to nitrate, respectively (Methods and Supplementary Information).

Biological transformations in forest canopies

At the ten sites, deposition of TN ranged from 3.4 to 15.8 kg $\text{ha}^{-1} \text{yr}^{-1}$ for BD and from 1.5 to 25.4 kg $\text{ha}^{-1} \text{yr}^{-1}$ for TF (Extended Data Table 1). Nitrogen fluxes were higher in TF than BD at most sites (Fig. 1), although the difference was significantly greater than zero only for NO_3^- -N and TN (Extended Data Fig. 1 and Extended Data Table 2). The canopies consistently retained all forms of nitrogen at the forest site in Sweden with the lowest nitrogen deposition, particularly when looking at the long-term changes in nitrogen fluxes (Extended Data Table 2).

Canopy release (TF > BD) is normally attributed to dry reactive nitrogen compounds previously deposited onto tree canopies being washed out during precipitation^{24–26}. However, the isotopic tracers ($\delta^{15}\text{N}$, $\delta^{18}\text{O}$ and $\Delta^{17}\text{O}$) indicated that NO_3^- in TF was a mixture of atmospheric and biological sources (Extended Data Fig. 2 and Extended Data Tables 3 and 4). We used a mass-balance approach based on $\Delta^{17}\text{O}$ (Methods) to determine that $68 \pm 25\%$ (s.d.) of the total NO_3^- in TF was from atmospheric deposition (f_{Atm}), and $32 \pm 25\%$ of the NO_3^- reaching the soil via TF was from canopy nitrification (f_{Bio}) (Fig. 2a), ranging across the gradient from 4% ($f_{\text{Bio}} = 0.04$) to 80% ($f_{\text{Bio}} = 0.8$). f_{Bio} was 0.37 ± 0.30 and 0.25 ± 0.18 for *F. sylvatica* and *P. sylvestris*, respectively (Fig. 2b), within the ranges reported in previous studies conducted on the same species in the UK³³ and in a *Quercus ilex* forest in Spain³⁴. Increases in f_{Bio} were associated with increases in TN (Extended Data Fig. 3 and Extended Data Table 5), suggesting that this process could be substrate-limited at lower inputs of atmospheric nitrogen.

Site-specific f_{Bio} was then used to partition TF NO_3^- -N fluxes into two sources: atmospheric deposition and biological transformation (hereon described as gross canopy nitrification, GCN). GCN contributed to adding between 0.40 and 4.97 kg N $\text{ha}^{-1} \text{yr}^{-1}$ for *F. sylvatica*

and between 0.21 and 3.23 kg N $\text{ha}^{-1} \text{yr}^{-1}$ for *P. sylvestris* to the NO_3^- -N derived from atmospheric deposition (Fig. 3a; Extended Data Table 4 provides the full range of values), with a mean (± 1 s.d., but adjusted for cross-site differences in TN deposition) of 1.77 ± 1.38 kg N $\text{ha}^{-1} \text{yr}^{-1}$. By comparison, the real (after correcting for GCN) contribution of atmospheric deposition to the TF NO_3^- -N fluxes averaged at an equivalent of 3.26 ± 1.13 kg N $\text{ha}^{-1} \text{yr}^{-1}$. Correction of the TF fluxes for the occurrence of GCN changed the balance of several forest canopies from being sources to apparent sinks of atmospheric NO_3^- -N (Fig. 3b), because the apparent release of NO_3^- -N from the canopy was often due to nitrification.

Microbial nitrifiers in the phyllosphere

The identification and quantification of microbial nitrifiers on foliar surfaces were supported by two independent DNA-based approaches: 16S rRNA gene metabarcoding and qPCR for functional genes. The analysis of 16S rRNA sequences confirmed the presence on foliar surfaces of previously known bacterial and archaeal autotrophic ammonia oxidizers (*Nitrosospira* and *Nitrospira*, and *Nitrososphaeraceae*, respectively) and bacterial autotrophic nitrite oxidizers (*Nitrospira*, *Nitrobacter* and *Burkholderia insulsa*)³⁷. The functional genes *amoA* and *nxrB* were detected in the phyllosphere (Fig. 4 and Extended Data Fig. 4). Archaeal *amoA* was more abundant ($P = 0.05$) than bacterial *amoA*, as previously observed in *Q. ilex* in the Mediterranean region³⁴, whereas only archaeal nitrifiers were present in the phyllosphere of *Criptomeria japonica*³⁸. The median difference between TF and BD for the functional genes involved in nitrification was significantly less than zero only for archaeal nitrifiers (V from a Wilcoxon test = 20, $P < 0.01$, Supplementary Fig. 1), suggesting that they could be more efficiently retained by tree canopies.

Microbial nitrifiers were also detected at sites where atmospheric nitrogen was retained in the canopy (Extended Data Table 2 and Extended Data Fig. 4), including three additional sites in Finland (Extended Data Table 1) that were added to the survey later, but for which estimates of f_{Bio} were not available (Methods). This finding does not necessarily indicate that canopy nitrification did not occur at these sites, but that NO_3^- -N is directly taken up by canopies³⁹ or that canopy nitrification is too low to be detected with our approach or, lastly, that the produced nitrate is consumed through denitrification. Indeed, microbial genes that encode enzymes involved in denitrification as

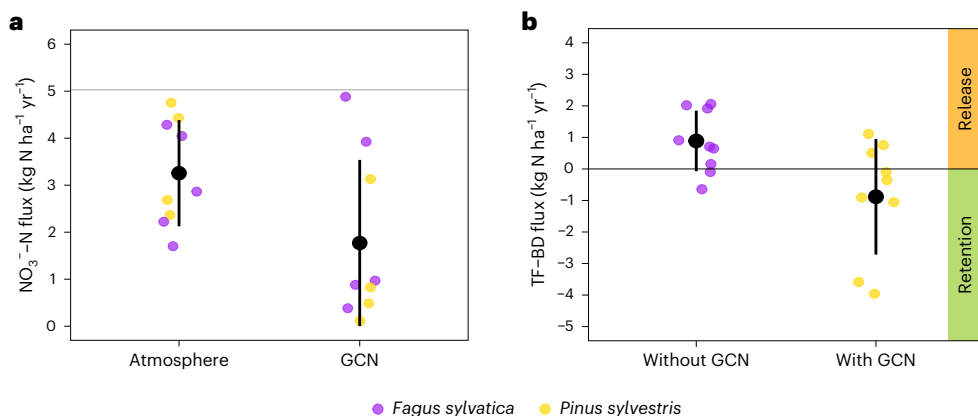


Fig. 3 | Partitioning between atmospheric deposition and GCN into TF nitrate fluxes and its ecological relevance. **a**, Partitioning of the NO_3^- -N TF fluxes into the two main sources (atmosphere and GCN, mean and s.d., $n=19$) obtained using f_{Bio} from Fig. 2 (more details are provided in the Methods). **b**, Difference between TF and BD for NO_3^- -N fluxes as measured (without GCN) and after accounting for GCN (with GCN). The grey line in **a** indicates the mean NO_3^- -N flux

in TF across all sites, that is, $5.03 \text{ kg N ha}^{-1} \text{ yr}^{-1}$. Each point is the mean calculated over two or three sampling dates ($n=19$; see Extended Data Table 4 for data). The orange and green rectangles to the right indicate the range of apparent release (source) and apparent retention (sink) of NO_3^- -N by forest canopies, respectively.

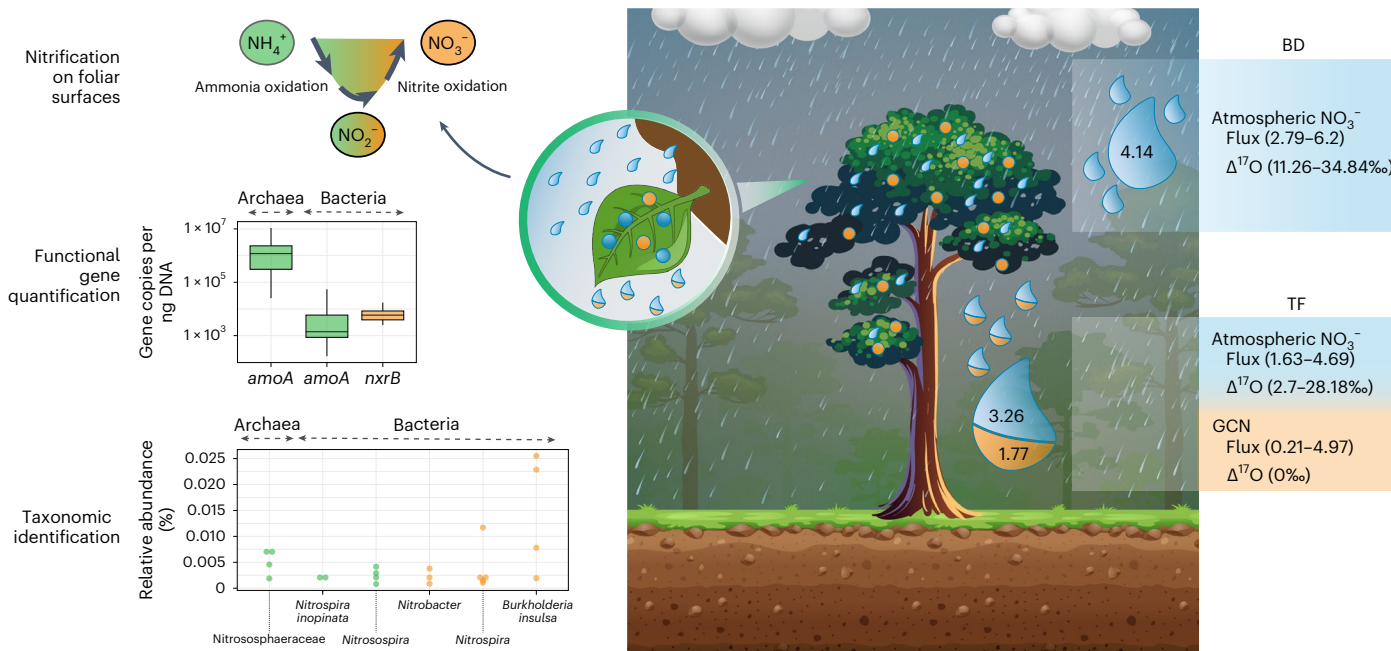


Fig. 4 | Overview of canopy nitrification and the occurrence of nitrifying microbes in the phyllosphere. The mean partitioning of TF water in atmospherically (light blue) and biologically (GCN, orange) (derived NO_3^- -N fluxes (both in $\text{kg N ha}^{-1} \text{ yr}^{-1}$), obtained using a mass-balance approach, is summarized in the cartoon on the right side of the panel. The range of values (minimum and maximum, all values are reported in Extended Data Tables 2 and 4) for the BD and TF fluxes and the $\Delta^{17}\text{O}$ in nitrate in the different components (BD, TF and nitrification) are also reported in the side boxes. For details on the mass-balance approach based on $\Delta^{17}\text{O}$ in nitrate to partition between GCN and atmospheric nitrate, see the Methods. The quantification of the main functional genes that encode for ammonia monooxygenase subunit A and nitrite oxidoreductase subunit B of bacteria (*amoA* AOB and *nxrB*) and archaea (*amoA*)

(AOA) catalysing the oxidation of ammonia to nitrite and of nitrite to nitrate, respectively, and the taxonomic identification of nitrifiers on the leaf surfaces across the investigated sites are shown on the left. Green and orange indicate genes and taxa associated with the pathways of ammonia or nitrite oxidation, respectively. Boxes represent the median (horizontal line) and the interquartile ranges of binned values (Q25, Q75), and the whiskers cover Q25 – 1.5(Q75 – Q25) to Q75 + 1.5(Q75 – Q25). Numbers of observations (n) for boxplots showing functional genes and taxonomic identification: Nitrosphaeraceae ($n=4$), *Nitrosopinka inopinata* ($n=2$), *Nitrosospira* ($n=4$); *Nitrobacter* ($n=3$), *Nitrospira* ($n=5$), *Burkholderia-Caballeronia-Paraburkholderia* ($n=4$), *amoA* from AOA ($n=26$), *amoA* from AOB ($n=22$), *nxrB* ($n=27$). Tree illustration adapted from ref. 23 under a Creative Commons license CC BY 4.0.

well as N_2 fixation were quantified on foliar surfaces (Supplementary Fig. 2), suggesting that nitrification may not be the only process occurring in the tree canopies of the investigated forests, as already observed in previous studies^{31,32,40}. Interestingly, N_2O emissions from tree canopies on a boreal forest were mostly associated with transport of N_2O

(derived from denitrification in the soil) through the transpiration stream⁴⁰. Molecular data from this study suggest that the process could potentially occur in the canopies too, although hypoxic-to-anoxic conditions are mostly required to promote denitrification, and these conditions may not be prevalent in the phyllosphere.

Ecological importance of canopy nitrification

Two lines of evidence support the argument that GCN is a key process in nitrogen cycling in forests. First, GCN, being processed in tree canopies, represents an input of dissolved unutilized NO_3^- that bypasses biological soil nitrification, thus contributing directly to potential pathway losses (leaching and denitrification). Field studies have reported lower net soil nitrification and NH_4^+ availability under pine and oak canopy covers compared to open areas, which was explained by a lower competition for NH_4^+ substrates between plants and nitrifiers in the former case⁴¹. Yet, our data indicate that GCN could contribute to reducing the input of atmospheric NH_4^+ to the soil. A data synthesis carried out in US forests showed that net soil nitrification can contribute to produce an average of $35 \text{ kg NO}_3^- \text{-N ha}^{-1} \text{ yr}^{-1}$, ranging from 0 (at the Harvard hardwood forest in Massachusetts) to $114.9 \text{ kg N ha}^{-1} \text{ yr}^{-1}$ (at the Fernow N-saturated mature forest in West Virginia)^{41,42}. Our GCN estimates were within the lower range of estimates of net soil nitrification from the above-mentioned meta-analysis. Most soil nitrification, however, represents internal cycling, as opposed to GCN, which represents a small (4.7% of total $\text{NO}_3^- \text{-N}$ from canopy plus mean soil nitrification, that is, $1.77/(1.77 + 35) \times 100$) but cumulative addition of NO_3^- to the ecosystem. Nevertheless, additional research, including both phyllospheric and soil nitrogen transformations, is needed to ascertain the absolute contribution of GCN to ecosystem nitrogen cycling.

Second, the ecological relevance of tree canopies in nutrient cycling will be underestimated if biological transformations by phyllospheric microbiota are neglected. Indeed, most forest canopies were $\text{NO}_3^- \text{-N}$ sinks rather than sources (for atmospheric deposition) when we accounted for the contribution of GCN to the measured TF $\text{NO}_3^- \text{-N}$ fluxes (Fig. 3b). The actual mean canopy retention (that is, the difference between TF and BD for $\text{NO}_3^- \text{-N}$ after accounting for GCN) was equivalent to $-1.03 \pm 1.78 \text{ kg N ha}^{-1} \text{ yr}^{-1}$, ranging from -4.76 to $1.33 \text{ kg N ha}^{-1} \text{ yr}^{-1}$. The $\text{NO}_3^- \text{-N}$ sink activity of tree canopies increased significantly with increasing TN deposition (Extended Data Fig. 5), indicating that this ecological process is relevant at low levels of nitrogen deposition^{39,43} but can also contribute to tree nutritional status at higher levels of atmospheric nitrogen inputs⁴⁴.

Our results force us to reconsider the current models used to estimate dry deposition. The canopy budget model²⁷ is based on the assumption that canopy exchange is the main process governing the uptake and release of ions when wet atmospheric deposition reaches forest canopies. For inorganic nitrogen, the uptake of NH_4^+ and/or H^+ by tree canopies is assumed to be balanced by the release of cations such as K^+ , Ca^{2+} and Mg^{2+} , whereas canopy NO_3^- uptake is proportional to NH_4^+ uptake²⁸. The lower $\text{NH}_4^+ \text{-N}$ fluxes in TF than BD would thus commonly be accounted for by canopy uptake²⁴, but we show that they could be due to transformations by epiphytic nitrifiers that bypass the trees. Furthermore, $\Delta^{17}\text{O}$ provided a robust estimate of the actual atmospheric $\text{NO}_3^- \text{-N}$ deposition, suggesting that attributing NO_3^- fluxes in TF only to the seldom-quantified fraction of dry deposition instead of GCN leads to overestimating atmospheric deposition in the oxidized form. We addressed possible limitations associated with the isotope approach considered in this study, which did not quantify nitrification directly on leaf surfaces but on collected forest water samples. One important limitation may be related to biological transformations occurring in water samples before their collection and/or during storage in the laboratory. However, a methodological test (Supplementary Text 1) was carried out at selected ICP Forest sites, where TF water samples were collected after the precipitation event and then subjected to different treatments (filtered and unfiltered water) and temperature levels (to simulate field conditions) for up to 85 days after collection. The results showed only small changes in NO_3^- concentrations and pH over time for different temperatures (Supplementary Tables 1 and 2 and Supplementary Figs. 3 and 4). The methodological test allowed the definition of a protocol for a robust estimate of water collection and

storage across all ICP Forest sites, as also employed at sites included in this study.

Our findings are relevant to the debate on widespread ecosystem nitrogen saturation versus oligotrophication¹⁸. The GCN flux we have shown could reduce the potential inputs of NH_4^+ to the soil and hence its preferential uptake (over NO_3^-) mediated by mycorrhizal associations for the investigated species, as reported in previous studies^{45,46}. We hypothesize that lower NH_4^+ availability could enhance tree–microbes competition and tree nitrogen demand under increasing levels of atmospheric CO_2 (refs. 18,47). However, this hypothesis should be tested in future studies, where the relevance of the GCN flux should be included in the well-investigated framework of inorganic and organic nitrogen uptake strategies and plant–microbe interactions in the rhizosphere^{48–50}. GCN can potentially contribute to increasing the highly soluble NO_3^- in the soil, and hence its loss via leaching and denitrification⁴². Studies at the watershed scale have shown greater export of microbiologically derived NO_3^- (attributed mostly to soil nitrification) with increasing nitrogen deposition in the case of nitrogen saturation^{51,52}. More studies are needed, however, to clarify the origin of the microbiologically derived NO_3^- , adding potential biological activities that are unseen in tree canopies.

The fact that this chronic net canopy retention of NO_3^- is more efficient under high atmospheric nitrogen loads also helps to explain why experimental nitrogen manipulations via soil fertilization generally underestimate the response of the tree carbon cycle to nitrogen availability under those same deposition conditions⁵³. More realistic nitrogen manipulation experiments are needed⁵⁴ if a more comprehensive understanding of the coupling between nitrogen and carbon cycling is to be achieved. Finally, our results highlight the need to integrate isotopic tracers to improve the current approaches used to estimate nitrogen deposition, to provide a more robust assessment of the CLs for policies aiming at limiting nitrogen pollution.

Online content

Any methods, additional references, Nature Portfolio reporting summaries, source data, extended data, supplementary information, acknowledgements, peer review information; details of author contributions and competing interests; and statements of data and code availability are available at <https://doi.org/10.1038/s41561-023-01364-3>.

References

1. Fowler, D. et al. The global nitrogen cycle in the twenty-first century. *Philos. Trans. R. Soc. B* **368**, 20130164 (2013).
2. Steffen, W. et al. Planetary boundaries: guiding human development on a changing planet. *Science* **347**, 1259855 (2015).
3. Magnani, F. et al. The human footprint in the carbon cycle of temperate and boreal forests. *Nature* **447**, 849–851 (2007).
4. Wang, R. et al. Global forest carbon uptake due to nitrogen and phosphorus deposition from 1850 to 2100. *Glob. Change Biol.* **23**, 4854–4872 (2017).
5. Galloway, J. N. et al. The nitrogen cascade. *BioScience* **53**, 341–356 (2003).
6. Sutton, M. A. et al. *The European Nitrogen Assessment* (Cambridge Univ. Press, 2011).
7. Keeler, B. L. et al. Linking water quality and well-being for improved assessment and valuation of ecosystem services. *Proc. Natl Acad. Sci. USA* **109**, 18619–18624 (2012).
8. Gu, B. et al. Abating ammonia is more cost-effective than nitrogen oxides for mitigating PM 2.5 air pollution. *Science* **374**, 758–762 (2021).
9. Aber, J. et al. Nitrogen saturation in temperate forest ecosystems. *BioScience* **48**, 921–934 (1998).
10. Bobbink, R. et al. Global assessment of nitrogen deposition effects on terrestrial plant diversity: a synthesis. *Ecol. Appl.* **20**, 30–59 (2010).

11. Pardo, L. H. et al. Effects of nitrogen deposition and empirical nitrogen critical loads for ecoregions of the United States. *Ecol. Appl.* **21**, 3049–3082 (2011).
12. Payne, R. J. et al. Impact of nitrogen deposition at the species level. *Proc. Natl Acad. Sci. USA* **110**, 984–987 (2013).
13. Nadelhoffer, K. J. et al. Nitrogen deposition makes a minor contribution to carbon sequestration in temperate forests. *Nature* **398**, 145–148 (1999).
14. Magill, A. H. et al. Ecosystem response to 15 years of chronic nitrogen additions at the Harvard Forest LTER, Massachusetts, USA. *For. Ecol. Manag.* **196**, 7–28 (2004).
15. Song, J. et al. A meta-analysis of 1,119 manipulative experiments on terrestrial carbon-cycling responses to global change. *Nat. Ecol. Evol.* **3**, 1309–1320 (2019).
16. Gundersen, P., Schmidt, I. K. & Raulund-Rasmussen, K. Leaching of nitrate from temperate forests—effects of air pollution and forest management. *Environ. Rev.* **14**, 1–57 (2006).
17. Craine, J. M. et al. Isotopic evidence for oligotrophication of terrestrial ecosystems. *Nat. Ecol. Evol.* **2**, 1735–1744 (2018).
18. Mason, R. E. et al. Evidence, causes and consequences of declining nitrogen availability in terrestrial ecosystems. *Science* **376**, eabh3767 (2022).
19. Zaehle, S. Terrestrial nitrogen-carbon cycle interactions at the global scale. *Philos. Trans. R. Soc. B* **368**, 20130125 (2013).
20. Terrer, C. et al. Nitrogen and phosphorus constrain the CO₂ fertilization of global plant biomass. *Nat. Clim. Chang.* **9**, 684–689 (2019).
21. Wang, S. et al. Recent global decline of CO₂ fertilization effects on vegetation photosynthesis. *Science* **370**, 1295–1300 (2020).
22. Vacher, C. et al. The phyllosphere: microbial jungle at the plant-climate interface. *Annu. Rev. Ecol. Evol. Syst.* **47**, 1–24 (2016).
23. Guerrieri, R., Templer, P. & Magnani, F. Canopy exchange and modification of nitrogen fluxes in forest ecosystems. *Curr. For. Rep.* **7**, 115–137 (2021).
24. Lindberg, S. E., Lovett, G. M., Richter, D. D. & Johnson, D. W. Atmospheric deposition and canopy interactions of major ions in a forest. *Science* **231**, 141–145 (1986).
25. Vanguelova, E. I. et al. Chemical fluxes in time through forest ecosystems in the UK—soil response to pollution recovery. *Environ. Pollut.* **158**, 1857–1869 (2010).
26. Ferretti, M. et al. On the tracks of nitrogen deposition effects on temperate forests at their southern European range—an observational study from Italy. *Glob. Chang. Biol.* **20**, 3423–3438 (2014).
27. Staelens, J., Houle, D., De Schrijver, A., Neirynck, J. & Verheyen, K. Calculating dry deposition and canopy exchange with the canopy budget model: review of assumptions and application to two deciduous forests. *Water Air Soil Pollut.* **191**, 149–169 (2008).
28. Adriaenssens, S. et al. Influence of canopy budget model approaches on atmospheric deposition estimates to forests. *Biogeochemistry* **116**, 215–229 (2013).
29. Vorholt, J. A. Microbial life in the phyllosphere. *Nat. Rev. Microbiol.* **10**, 828–840 (2012).
30. Kembel, S. W. et al. Relationships between phyllosphere bacterial communities and plant functional traits in a neotropical forest. *Proc. Natl Acad. Sci. USA* **111**, 13715–13720 (2014).
31. Fürnkranz, M. et al. Nitrogen fixation by phyllosphere bacteria associated with higher plants and their colonizing epiphytes of a tropical lowland rainforest of Costa Rica. *ISME J.* **2**, 561–570 (2008).
32. Bowatte, S., Newton, P. C., Brock, S., Theobald, P. & Luo, D. Bacteria on leaves: a previously unrecognised source of N₂O in grazed pastures. *ISME J.* **9**, 265–267 (2015).
33. Guerrieri, R., Vanguelova, E. I., Michalski, G., Heaton, T. H. E. & Mencuccini, M. Isotopic evidence for the occurrence of biological nitrification and nitrogen deposition processing in forest canopies. *Glob. Chang. Biol.* **21**, 4613–4626 (2015).
34. Guerrieri, R. et al. Partitioning between atmospheric deposition and canopy microbial nitrification into throughfall nitrate fluxes in a Mediterranean forest. *J. Ecol.* **108**, 626–640 (2020).
35. Bobbink, R., Loran, C. & Tomassen, H. *Review and Revision of Empirical Critical Loads and Dose–Response Relationships* (German Environment Agency, 2022).
36. Michalski, G., Scott, Z., Kabiling, M. & Thiemens, M. H. First measurements and modeling of Δ¹⁷O in atmospheric nitrate. *Geophys. Res. Lett.* **30**, 1870 (2003).
37. Kuypers, M. M. M., Marchant, H. K. & Kartal, B. The microbial nitrogen-cycling network. *Nat. Rev. Microbiol.* **16**, 263–276 (2018).
38. Watanabe, K. et al. Microbial nitrification in throughfall of a Japanese cedar associated with archaea from the tree canopy. *SpringerPlus* **5**, 1596 (2016).
39. Ferrareto, D. et al. Forest canopy nitrogen uptake can supply entire foliar demand. *Funct. Ecol.* **36**, 933–949 (2022).
40. Machacova, K. et al. *Pinus sylvestris* as a missing source of nitrous oxide and methane in boreal forest. *Sci. Rep.* **6**, 23410 (2016).
41. Fenn, M. E., Poth, M. A., Terry, J. D. & Blubaugh, T. J. Nitrogen mineralization and nitrification in a mixed-conifer forest in southern California: controlling factors, fluxes and nitrogen fertilization response at a high and low nitrogen deposition site. *Can. J. Res.* **35**, 1464–1486 (2005).
42. Fang, Y. et al. Microbial denitrification dominates nitrate losses from forest ecosystems. *Proc. Natl Acad. Sci. USA* **112**, 1470–1474 (2015).
43. Houle, D., Marty, C. & Duchesne, L. Response of canopy nitrogen uptake to a rapid decrease in bulk nitrate deposition in two eastern Canadian boreal forests. *Oecologia* **177**, 29–37 (2015).
44. Schwarz, M. T. et al. More efficient aboveground nitrogen use in more diverse Central European forest canopies. *For. Ecol. Manag.* **313**, 274–282 (2014).
45. Gessler, A. et al. Field and laboratory experiments on net uptake of nitrate and ammonium by the roots of spruce (*Picea abies*) and beech (*Fagus sylvatica*) trees. *N. Phytol.* **138**, 275–285 (1998).
46. Gruffman, L., Jamtgard, S. & Nasholm, T. Plant nitrogen status and co-occurrence of organic and inorganic nitrogen sources influence root uptake by Scots pine seedlings. *Tree Physiol.* **34**, 205–213 (2014).
47. Penuelas, J. et al. Increasing atmospheric CO₂ concentrations correlate with declining nutritional status of European forests. *Commun. Biol.* **3**, 125 (2020).
48. Schimel, J. P. & Bennett, J. Nitrogen mineralization: challenges of a changing paradigm. *Ecology* **85**, 591–602 (2004).
49. Khokon, A. M., Janz, D. & Polle, A. Ectomycorrhizal diversity, taxon-specific traits and root N uptake in temperate beech forests. *N. Phytol.* **239**, 739–775 (2023).
50. Baldrian, P., López-Mondéjar, R. & Kohout, P. Forest microbiome and global change. *Nat. Rev. Microbiol.* **21**, 487–501 (2023).
51. Rose, L. A., Elliott, E. M. & Adams, M. B. Triple nitrate isotopes indicate differing nitrate source contributions to streams across a nitrogen saturation gradient. *Ecosystems* **18**, 1209–1223 (2015).
52. Huang, S. et al. Multiyear measurements on Δ¹⁷O of stream nitrate indicate high nitrate production in a temperate forest. *Environ. Sci. Technol.* **54**, 4231–4239 (2020).
53. Schulte-Uebbing, L. F., Ros, G. H. & de Vries, W. Experimental evidence shows minor contribution of nitrogen deposition to global forest carbon sequestration. *Glob. Chang. Biol.* **28**, 899–917 (2022).
54. Bebbet, D. P. The gap between atmospheric nitrogen deposition experiments and reality. *Sci. Total Environ.* **801**, 149774 (2021).

Publisher's note Springer Nature remains neutral with regard to jurisdictional claims in published maps and institutional affiliations.

Open Access This article is licensed under a Creative Commons Attribution 4.0 International License, which permits use, sharing, adaptation, distribution and reproduction in any medium or format, as long as you give appropriate credit to the original author(s) and the source, provide a link to the Creative Commons license, and indicate if changes were made. The images or other third party material in this

article are included in the article's Creative Commons license, unless indicated otherwise in a credit line to the material. If material is not included in the article's Creative Commons license and your intended use is not permitted by statutory regulation or exceeds the permitted use, you will need to obtain permission directly from the copyright holder. To view a copy of this license, visit <http://creativecommons.org/licenses/by/4.0/>.

© The Author(s) 2024

¹Department of Agricultural and Food Sciences, University of Bologna, Bologna, Italy. ²CREAF, Cerdanya del Vallès, Barcelona, Spain. ³Centre of Advanced Studies of Blanes, CEAB-CSIC, Spanish Council for Scientific Research, Blanes, Spain. ⁴CSIC, Global Ecology Unit CREAF-CSIC-UAB, Barcelona, Spain. ⁵Servei de Genòmica i Bioinformàtica, IBB-Parc de Recerca UAB – Mòdul B, Universitat Autònoma de Barcelona, Bellaterra, Barcelona, Spain.

⁶Department of Pharmacy and Biotechnology, University of Bologna, Bologna, Italy. ⁷Universidad de Navarra, Instituto de Biodiversidad y Medioambiente BIOMA, Pamplona, Spain. ⁸Northwestern Forest Research Institute, Göttingen, Germany. ⁹IVL Swedish Environmental Research Institute, Gothenburg, Sweden. ¹⁰Natural Resources Institute Finland (Luke), Oulu, Finland. ¹¹National Research Council of Italy, Institute of BioEconomy (CNR-IBE), Florence, Italy. ¹²Department of Earth, Atmospheric, and Planetary Sciences, Purdue University, West Lafayette, IN, USA. ¹³ONF, Office National des Forêts, Departement Recherche et Développement, Fontainebleau, France. ¹⁴WSL, Swiss Federal Institute for Forest, Snow and Landscape Research, Birmensdorf, Switzerland. ¹⁵Centre for Forest Protection, Forest Research, Farnham, UK. ¹⁶Research Institute for Nature and Forest (INBO), Geraardsbergen, Belgium.

¹⁷National Institute for Environmental Studies, Tsukuba, Ibaraki, Japan. ¹⁸ICREA, Barcelona, Spain. ✉ e-mail: r.guerrieri@unibo.it

Methods

Investigated sites and quantification of atmospheric nitrogen deposition

Ten forested sites within the Level II ICP Forests network (<http://icp-forests.net/>)⁵⁵ composed of the two most common European tree species (*Fagus sylvatica* L. and *Pinus sylvestris* L.) were selected to span a range of climates (Fig. 1a)⁵⁶ and nitrogen-deposition conditions (Extended Data Table 1). Specifically, sites were considered at low or high levels of nitrogen deposition if the sum of the $\text{NH}_4^+ - \text{N}$ and $\text{NO}_3^- - \text{N}$ fluxes in TF was below or above the CL, respectively. The empirical CL is $10 - 15 \text{ kg N ha}^{-1} \text{ yr}^{-1}$ according to the summary table 9.2 in ref. 35. Atmospheric deposition, foliar nutrients and tree growth, among other parameters, have been continuously measured at sites in the ICP Forests monitoring network since 1995. The flux of atmospheric nitrogen deposition at these sites was quantified by measuring NH_4^+ and NO_3^- concentrations in water collected in open fields outside the forests (BD) and beneath tree canopies (TF). At each site, between one and four collectors were used for BD, and 10–16 TF collectors were placed within the monitored plots, following either a systematic or random distribution, to capture the spatial variability of the canopy cover. In addition to the collectors for BD, wet-only deposition was determined at one site (in Belgium) by employing collectors whose lid automatically opened at the start of rain and closed 10–15 min after the rain ended, to avoid collecting ions from dry deposition. Bottles in which water samples were collected were placed in PVC pipes to minimize algal growth and biological transformations in the samples (Supplementary Text 1). The samples were collected and processed following a protocol harmonized across all sites, as described in the ICP Forests manual⁵⁷. Briefly, the samples were normally collected weekly (once a week), biweekly (once every 2 weeks) or monthly (depending on the site and precipitation). An aliquot of the total volume of BD and TF water collected, between 100 and 200 ml (depending on the site), was filtered through acetate cellulose membranes with a pore size of 0.45 µm and used for measuring NH_4^+ and NO_3^- concentrations (in mg l⁻¹), which were then used to quantify the monthly fluxes of deposition of $\text{NH}_4^+ - \text{N}$ and $\text{NO}_3^- - \text{N}$ based on the volume of water collected^{25,58,59}. Annual BD and TF fluxes were obtained as sums of monthly fluxes and are expressed as $\text{NH}_4^+ - \text{N}$, $\text{NO}_3^- - \text{N}$ and TN, with TN obtained as the sum of both inorganic forms of nitrogen ($\text{NH}_4^+ - \text{N}$ and $\text{NO}_3^- - \text{N}$) and organic nitrogen. The total deposition of nitrogen onto forests is assumed to be typically a factor of one to two times higher than TF fluxes⁵⁹ due to the deposition of dry reactive nitrogen compounds (particulate and gaseous) onto tree canopies. The deposition of these reactive compounds, washed out during precipitation, is larger in forests than in the open field because of the larger surface area and resistance of canopies compared with open field receptors. However, here we only focused on measured water fluxes below the forest canopy and outside the forest, as dry deposition is not extensively and separately measured across all the ICP Forests sites.

Collection of foliar and water samples

BD and TF water were collected on two or three sampling dates during summer of 2016 at each of the ten sites (Supplementary Table 3). The sampling was originally planned for August and September, but it was extended from July to October 2016 due to the low precipitation at most of the sites in August. All water samples were transported to the laboratory on the day of collection and stored at 2–4 °C in the dark until processing, as described earlier. The remaining water collected on a sampling date was filtered through sterilized mixed cellulose membrane filters with a pore size of 0.22 µm (S-Pak™ Membranes, Merck) to collect microorganisms for the DNA-based molecular analyses (Supplementary Text 2), which were stored at –20 °C until DNA extraction. At each site, 1–3 and 10–12 filters were used to filter the BD and TF water samples, respectively. The filtered water was stored at 2–4 °C in the dark until preparation for isotopic analyses. At each

site, foliar samples were collected from five trees where TF collectors were located, chosen among those already considered for nutrient analysis in the ICP Forests network. Three additional sites in Finland were added later to increase the number of sites at the lower range of nitrogen deposition (that is, <5 kg ha⁻¹ yr⁻¹, Supplementary Table 1). Three shoots from each tree were sampled in the upper, middle and lower third of the canopy. Professional tree climbers collected the samples in August 2016 (except in Sweden and Finland, where the samples were collected in October 2016 and August 2017, respectively). To avoid contact between the foliage and the ground (and possible contamination with soil microbes), shoots were sampled from the canopy and directly placed in labelled sterilized bags, which were sealed when the tree climber was still in the canopy. The sealed bags were then dropped to the forest floor and immediately placed in a box containing dry ice. The foliar samples were stored in the laboratory at –20 °C until the extraction of microbial DNA.

Analyses of stable isotopes in nitrate and partitioning between atmospheric and biological sources for TF fluxes

The site-composite samples of BD and TF water from each sampling date were used for the measurements of the stable isotopes of NO_3^- . The samples were conveyed through an anion-exchange resin (AG1-X8, analytical grade, 20–50 mesh, chloride form) to retain NO_3^- , which was then eluted from the resin using 20 ml of 1 M KBr and processed using bacterial reduction and thermal decomposition to measure the $^{18}\text{O}/^{16}\text{O}$, $^{17}\text{O}/^{16}\text{O}$ and $^{15}\text{N}/^{14}\text{N}$ isotopic ratios, as described in ref. 34. The oxygen and nitrogen isotopic ratios in the samples were expressed in parts per thousand (‰) relative to international standards (Vienna Standard Mean Ocean Water (VSMOW)) and atmospheric N_2 , respectively, to obtain the oxygen ($\delta^{18}\text{O}$ and $\delta^{17}\text{O}$) and nitrogen ($\delta^{15}\text{N}$) isotopic compositions. The long-term analytical precisions were ±0.2‰ ($\delta^{18}\text{O}$ and $\delta^{15}\text{N}$) and ±0.5‰ ($\delta^{17}\text{O}$). The isotopic composition values are presented in Extended Data Tables 3 and 4.

The excess ^{17}O in atmospheric NO_3^- , that is, $\Delta^{17}\text{O}$ (expressed as $\Delta^{17}\text{O} = \delta^{17}\text{O} - 0.52 \times \delta^{18}\text{O}$), unequivocally estimates the proportion of NO_3^- derived from atmospheric deposition, because it is determined by mass-independent fractionations during the photochemical production of NO_3^- in the atmosphere³⁶. The fraction of NO_3^- from biological transformation (that is, nitrification, f_{Bio}) in the canopy relative to the fraction from atmospheric deposition (f_{Atm}) was assessed using a mass-balance approach based on $\Delta^{17}\text{O}$ values³⁶ measured in BD and TF, as described elsewhere^{33,34,60}. Briefly, we started with

$$\Delta^{17}\text{O}_{\text{TF}} = f_{\text{Bio}} (\Delta^{17}\text{O}_{\text{Bio}}) + f_{\text{Atm}} (\Delta^{17}\text{O}_{\text{Atm}}) \quad (1)$$

where $\Delta^{17}\text{O}_{\text{TF}}$, $\Delta^{17}\text{O}_{\text{Bio}}$ and $\Delta^{17}\text{O}_{\text{Atm}}$ are the values of $\Delta^{17}\text{O}$ in TF water NO_3^- , nitrification-derived NO_3^- and atmosphere-derived NO_3^- , respectively, and f_{Bio} and f_{Atm} are the two unknown NO_3^- fractions from the two sources (biological and atmospheric), whose sum should be 1:

$$f_{\text{Bio}} + f_{\text{Atm}} = 1 \quad (2)$$

f_{Atm} included the fractions of both the wet (f_{Wet}) and dry (f_{Dry}) NO_3^- depositions washed from the canopy and/or taken up by leaves (f_{U}), that is, $f_{\text{Atm}} = f_{\text{Wet}} + f_{\text{Dry}} - f_{\text{U}}$. Assuming that $\Delta^{17}\text{O}_{\text{Bio}} = 0$ (ref. 36) and that the $\Delta^{17}\text{O}$ of NO_3^- in BD represented both wet and dry NO_3^- deposition⁶¹, equation (1) can be reduced to

$$f_{\text{Atm}} = \frac{\Delta^{17}\text{O}_{\text{TF}}}{\Delta^{17}\text{O}_{\text{BD}}} \quad (3)$$

which can then be used in equation (2) to obtain f_{Bio} as

$$f_{\text{Bio}} = 1 - f_{\text{Atm}} \quad (4)$$

f_{Bio} and f_{Atm} were then used to calculate the NO_3^- -N flux derived from canopy nitrification (GCN) and the actual atmospheric NO_3^- -N (after accounting for GCN) using an approach similar to that applied at the watershed scale⁵² (Extended Data Table 4), that is, by multiplying the measured NO_3^- -N TF flux by f_{Bio} and f_{Atm} . The fact that dry nitrogen deposition was not included in the study does not affect the estimate of GCN, as the latter is calculated from TF fluxes.

Genetic analyses

For the phyllosphere, of the five trees from which shoots ($n = 3$) were originally collected, only three were used for the analysis of phyllospheric microbiota, and the remaining two were used when foliar samples did not look healthy (for example, in the Collelongo site in Italy) and/or when not enough microbial DNA (for example, in the forest site in Sweden) could be collected. Epiphytic microbial DNA was obtained from 5–6 g (for *F. sylvatica*) and 8–10 g (for *P. sylvestris*) of foliage randomly collected from each of the three shoots sampled per tree and placed (as a composite sample for each tree) in sterile 50-ml Falcon tubes. Thirty-five millilitres of 1:50 diluted Redford buffer wash solution (1 M Tris-HCl, 0.5 M Na ethylenediaminetetraacetic acid (EDTA) and 1.2% cetyltrimethylammonium bromide (CTAB)³⁵) was added to each tube, which was then stirred for 5 min. The washing solution was transferred to a second sterile 50-ml tube and centrifuged at 3,000g for 30 min. The pellet was transferred to 2-ml MO BIO PowerSoil bead-beating tubes for DNA extraction, which was conducted following the manufacturer's instructions (DNeasy PowerSoil Kit, Qiagen, Benelux BV; previously the PowerSoil DNA isolation kit from Mo Bio laboratories). The microbial DNA was quantified using a NanoDrop spectrophotometer (Thermo Fisher Scientific). For the water samples, filters for the genetic analyses were cut into pieces and transferred to 2-ml MO BIO PowerSoil bead-beating tubes. Microbial DNA was extracted from all samples using an MO BIO PowerSoil DNA isolation kit (MO BIO) following the manufacturer's instructions, as described for the phyllosphere.

Aliquots of microbial DNA, obtained as described above, were used to (1) prepare amplicon libraries for Illumina 16S rRNA gene sequencing and (2) quantify the functional genes involved in nitrification using qPCR analyses (expressed as the number of copies of the gene per nanogram of microbial DNA extracted from a sample), that is, genes that encode for ammonia monooxygenase subunit A (*amoA*) and nitrite oxidoreductase subunit B (*nxrB*) catalysing the oxidation of ammonia to nitrite and nitrite to nitrate, respectively. More details for those analyses are provided in Supplementary Text 2.

Statistical analyses

We used *t*-tests to assess whether the mean of the difference between TF and BD for nitrogen deposition in the form of NO_3^- -N and TN differed from zero. The data for determining the difference between TF and BD for NH_4^+ -N and the microbial functional genes (*amoA* AOA, *amoA* AOB and *nxrB*) were not normally distributed, so we used the non-parametric Wilcoxon–Mann–Whitney test to test the null hypothesis that the median of the difference between BD and TF differed significantly from zero. Simple regression analyses were conducted to identify the relationships between f_{Bio} or GCN and the data for N deposition. All statistical analyses were conducted in R⁶² using the following packages: 'stats'⁶² for the *t*- and Wilcoxon–Mann–Whitney, 'car'⁶³ for linear regression analyses and 'ggplot2'⁶⁴ for the figures. Finally, the package 'rnaturalearth'⁶⁵ was used for producing the map in Fig. 1a.

Data availability

All data used in the main figures, Extended Data figures and Supplementary figures have been deposited in Zenodo (<https://doi.org/10.5281/zenodo.10302622>). Genetic data from 16S sequence analyses are available in the Sequence Reading Archive at the National Center for Biotechnology Information under accession no. PRJNA859654.

Code availability

The coding involved in this study is for statistical analyses, using the specific packages described in the 'Statistical analyses' section.

References

55. de Vries, W. Intensive monitoring of forest ecosystems in Europe 1. Objectives, set-up and evaluation strategy. *Forest Ecol. Manag.* **174**, 77–95 (2003).
56. Haylock, M. R. et al. A European daily high-resolution gridded dataset of surface temperature and precipitation. *J. Geophys. Res.* **113**, D20119 (2008).
57. Clarke, N. et al. UNECE ICP Forests Programme Co-ordinating Centre: *Manual on Methods and Criteria for Harmonized Sampling, Assessment, Monitoring and Analysis of the Effects of Air Pollution on Forests Part XIV* (Thünen Institute of Forest Ecosystems, 2020); <http://www.icp-forests.org/Manual.htm>
58. Thimonier, A. et al. Total deposition of nitrogen in Swiss forests: comparison of assessment methods and evaluation of changes over two decades. *Atmos. Environ.* **198**, 335–350 (2019).
59. Waldner, P. et al. Detection of temporal trends in atmospheric deposition of inorganic nitrogen and sulphate to forests in Europe. *Atmos. Environ.* **95**, 363–374 (2014).
60. Riha, K. M. et al. High atmospheric nitrate inputs and nitrogen turnover in semi-arid urban catchments. *Ecosystems* **17**, 1309–1325 (2014).
61. Nelson, D. M. et al. Triple oxygen isotopes indicate urbanization affects sources of nitrate in wet and dry atmospheric deposition. *Atmos. Chem. Phys.* **18**, 6381–6392 (2018).
62. R Core Team. R: a language and environment for statistical computing. *R Foundation for Statistical Computing* <https://www.R-project.org/> (2020).
63. Fox, J. & Weisberg, S. *An R Companion to Applied Regression* 3rd edn (Sage, 2019).
64. Wickham, H. *ggplot2: Elegant Graphics for Data Analysis* (Springer, 2016).
65. Massicotte P. & South, A. rnaturalearth: World Map Data from Natural Earth. R package version 0.3.4. CRAN <https://CRAN.R-project.org/package=rnaturalearth> (2023).
66. Kendall, C., Elliott, E. M. & Wankel, S. D. in *Stable Isotopes in Ecology and Environmental Science* (eds Michener, R. & Lajtha, K.) 375–449 (Blackwell, 2007).
67. Marchetto, A., Arisci, S., Tartari, G. A., Balestrini, R. & Tait, D. Stato ed evoluzione temporale della composizione chimica delle deposizioni atmosferiche nelle aree forestali della rete CONECOFOR. *Forest@* **11**, 72–85 (2014).
68. Bussotti, F., Pancrazi, M., Matteucci, G. & Gerosa, G. Leaf morphology and chemistry in *Fagus sylvatica* (beech) trees as affected by site factors and ozone: results from CONECOFOR permanent monitoring plots in Italy. *Tree Physiol.* **25**, 211–219 (2005).
69. Flechard, C. R. et al. Carbon–nitrogen interactions in European forests and semi-natural vegetation—Part 1: fluxes and budgets of carbon, nitrogen and greenhouse gases from ecosystem monitoring and modeling. *Biogeosciences* **17**, 1583–1620 (2020).

Acknowledgements

This study was supported by EU funding from the MSCA individual fellowship (NITRIPHYLL no. 705432; to R.G.) and from European Research Council Synergy grant ERC-2013-SyG610028-IMBALANCE-P (to J.P.), and by funding from the Flemish government, Research Institute for Nature and Forest (INBO) (to A.V.). J.C. and E.O.C. were supported by the grant INTERACTOMA RTI2018-101205-B-I00 from the Spanish Agency of Research (AEI-MICINN) and European funding (ERDF). We are grateful for the support provided by M. Schmitt, N. Hajjar and O. Schramm from WSL (CH), J. Brunt from FR (UK) and

Y. De Bodt from INBO (Belgium) during fieldwork and filtering of the water. This study greatly benefited from the large efforts of the site PIs and collaborators coordinating long-term monitoring within the ICP Forests network. The measurements within The Swedish Throughfall Monitoring Network (SWETHRO) are mainly funded by various regional air quality protection associations, county administrative boards and the Swedish Environmental Protection Agency. We acknowledge the E-OBS dataset from the EU-FP6 project UERRA (<https://www.uerra.eu>) and the Copernicus Climate Change Service, and the data providers in the ECA&D project (<https://www.ecad.eu>).

Author contributions

R.G., M.M. and J.P. conceived the study. R.G. and M.M. led the experimental design. A.V., E.V., P.W., A.T., D.E., S.H., P.M., A.-J.L., M.N. and G. Matteucci were responsible for collecting foliar and water samples, filtering and chemically analysing water for quantifying fluxes of nitrogen deposition, and collating and validating forest and environmental data. R.G. was responsible for extracting microbial DNA from foliar and water samples, with the supervision of A.B. and S.M., and for processing the water through anionic resins for the isotopic analyses. G. Michalski conducted stable isotope analyses of nitrate. A.B. sequenced the DNA using an Illumina platform, and S.M. conducted the qPCR analyses, with support from M.W. J.C. processed the raw DNA sequences obtained from the Illumina platform and conducted bioinformatic analyses with the support of E.O.C. R.G. was responsible for processing the isotopes and functional genes data, statistical analyses and generating all the figures, with support from J.C. (for the map in Fig. 1 and for Fig. 4). S.T. and M.C. provided

support for the preliminary confocal microscopy observations before processing the samples for microbial DNA extraction. N.K. and H.F. set up the experiment described in Supplementary Text 1 and provided the data shown in Supplementary Figs. 3 and 4. R.G. and M.M. prepared the original draft of the manuscript, with input from J.C., E.O.C., S.M. and J.P. All authors discussed the results and commented on the manuscript.

Competing interests

The authors declare no competing interests.

Additional information

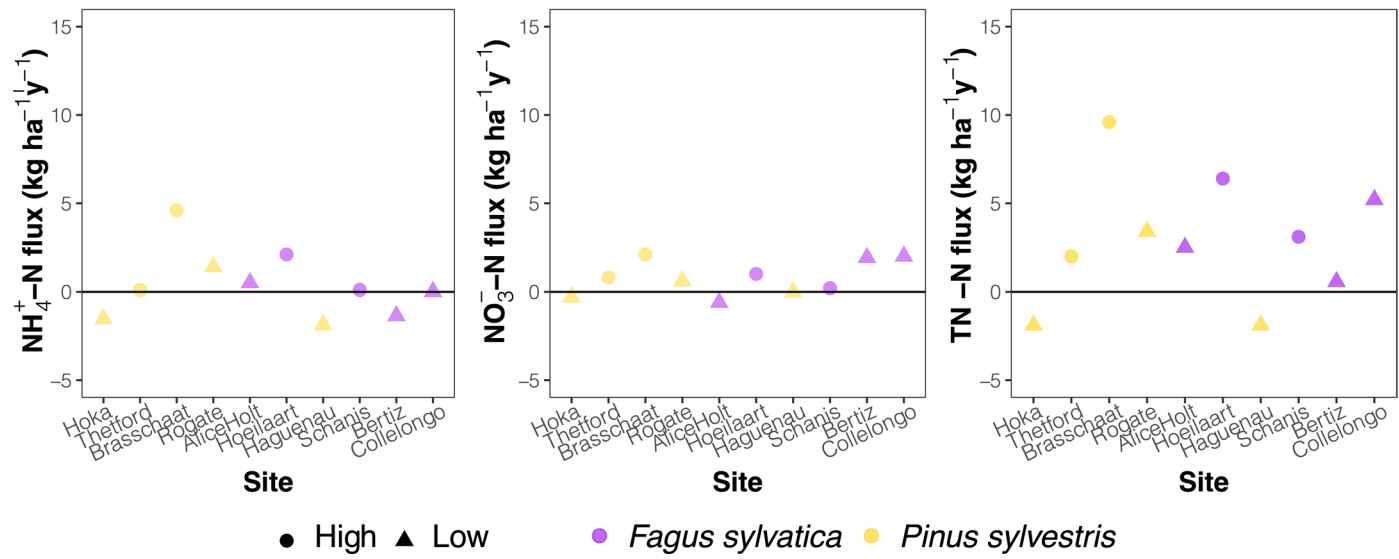
Extended data is available for this paper at <https://doi.org/10.1038/s41561-023-01364-3>.

Supplementary information The online version contains supplementary material available at <https://doi.org/10.1038/s41561-023-01364-3>.

Correspondence and requests for materials should be addressed to Rossella Guerrieri.

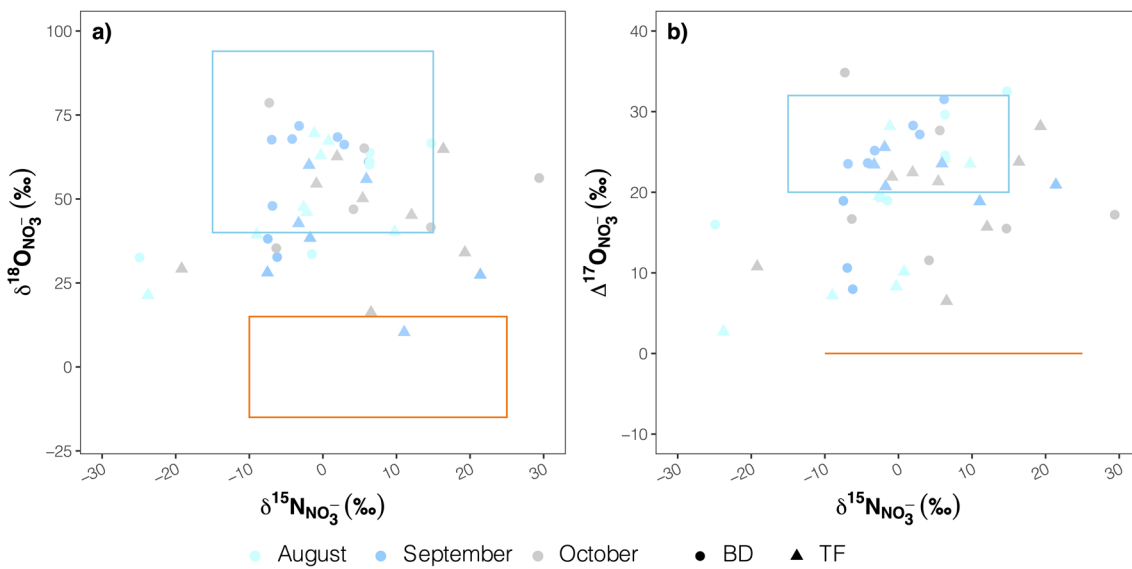
Peer review information *Nature Geoscience* thanks Shun Li, Zhongjie Yu and the other, anonymous, reviewer(s) for their contribution to the peer review of this work. Primary Handling Editor: Xujia Jiang, in collaboration with the *Nature Geoscience* team.

Reprints and permissions information is available at www.nature.com/reprints.



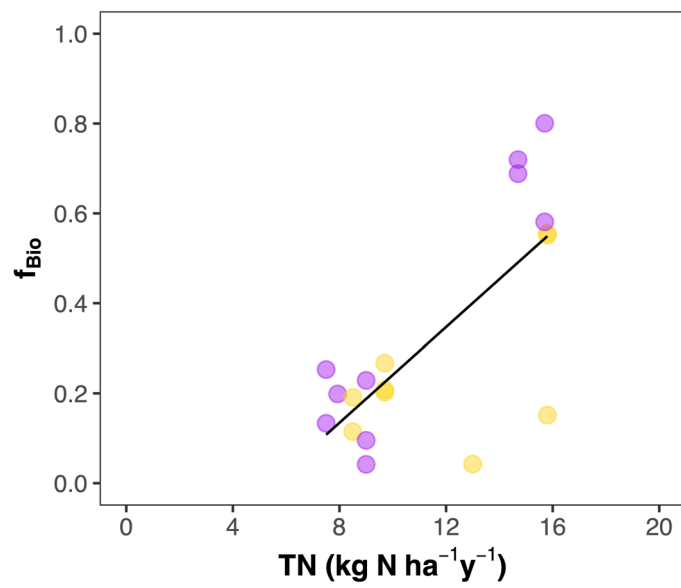
Extended Data Fig. 1 | Nitrogen fluxes expressed as difference between TF and BD across the investigated sites. Differences between throughfall (TF) and bulk deposition (BD) for each form of nitrogen compounds measured in 2016 at the 10 sites in the study. Different shapes indicate sites at low or high levels

of N deposition, if the sum of $\text{NH}_4^+ \text{-N}$, $\text{NO}_3^- \text{-N}$ fluxes in TF was below or above the critical nitrogen loads (CL), respectively. Empirical CL is 10–15 kg N ha⁻¹ y⁻¹ according to Bobbink et al.³⁵ (Table 9.2).



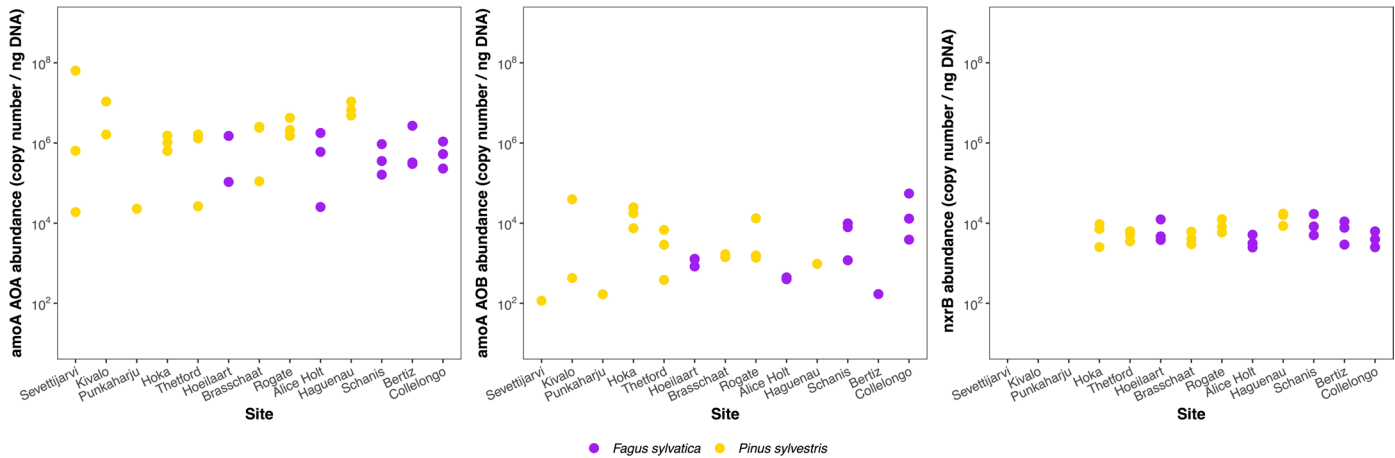
Extended Data Fig. 2 | Stable oxygen and nitrogen isotope compositions of nitrate in forest water samples. **a,b,** Dual isotope plots showing the distribution of $\delta^{18}\text{O}$ vs. $\delta^{15}\text{N}$ (a) and $\Delta^{17}\text{O}$ vs. $\delta^{15}\text{N}$ (b) measured on NO_3^- in forest water samples collected on two or three sampling dates, reported in Supplementary Table 3 and Extended Data Tables 3, 4. The blue and orange boxes indicate the published

ranges of isotopic values for atmospherically and biologically derived NO_3^- , respectively, reported by Kendall et al.⁶⁶. Note that the figure reports raw measurements for each sampling date and that the accurate partitioning of the fractions of biologically derived NO_3^- requires examining the ratios of the individual BD-TF pairs in the mass balance approach (see Methods).



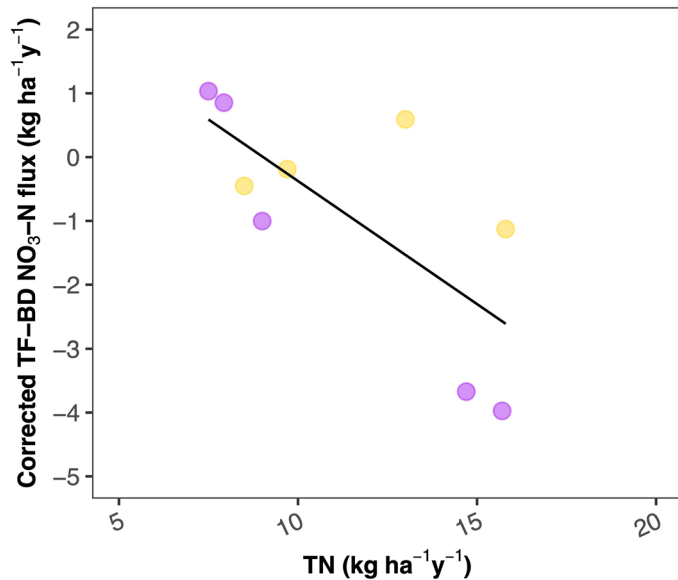
Extended Data Fig. 3 | Relationship between biological fraction of nitrate and atmospheric deposition. Relationship between the fraction of nitrate derived from biological transformation in tree canopies (f_{Bio}) and the annual bulk deposition (BD) of total nitrogen (TN, that is, inorganic + dissolved organic nitrogen deposition) in 2016. We plot f_{Bio} values obtained from each sampling

period (Supplementary Table 3) as listed in the Extended Data Table 4, while annual values for TN in BD were considered (as reported in the Extended Data Table 1). See Extended Data Table 5 for the statistical results of the linear regression analysis.



Extended Data Fig. 4 | Abundance of the microbial functional genes involved in the canopy nitrification. Abundance of the archaeal and bacterial genes that encode for ammonia monooxygenase subunit A (*amoA* AOA and *amoA* AOB, respectively) and the bacterial gene encoding for nitrite oxidoreductase (*nxrB*). Abundance (y-axis) is expressed as copy number of a given gene relative to nanograms of extracted DNA from foliar surfaces. All values were log-10 transformed. The sites on the x-axis follow a latitudinal order from north to

south. Number of observations (n) for each functional gene is: n=3 at each site, except for *amoA* AOB in Bertiz, Haguenau, Savettijarvi (n=1) and Brasschaat and Kivalo (n=2), for *amoA* AOA in Kivalo and Hoeilaart (n=2) and for *nxrB*. The lower number of observations at those sites were either related to low microbial DNA extracted from the phyllosphere or to copy number lower than the minimum values of 100.



Extended Data Fig. 5 | Relationship between TF-BD difference (after correction for canopy nitrification) and nitrogen deposition. Relationship between the difference between throughfall (TF) and bulk deposition (BD) of nitrate (NO_3^- -N) after correction for gross canopy nitrification and bulk

deposition of total nitrogen (TN). Linear regression indicated significant relationships between the two variables (slope: -0.4 ± 0.14 , $R^2 = 0.53$, $p = 0.03$), which was stronger when the interaction term $\text{TN} \times \text{Species}$ was also included ($R^2 = 0.92$, $p < 0.01$).

Extended Data Table 1 | Description of the sites included in the study. Latitude (Lat), longitude (Long), annual mean temperature (T_a), total annual precipitation (P_a), and annual depositions of NH_4^+ -N, NO_3^- -N, and total N (TN, that is deposition of inorganic + dissolved organic nitrogen) refer to data from 2016. BD and TF indicate bulk deposition and throughfall, respectively. Tree species are *Pinus sylvestris* (PS) and *Fagus sylvatica* (FS). Sites were considered at low or high levels of N deposition if the sum of NH_4^+ -N, NO_3^- -N fluxes in TF was below or above the critical nitrogen loads (CL), respectively. Empirical CL is 10–15 kg N $\text{ha}^{-1} \text{y}^{-1}$ according to Bobbink et al.³⁵, Table 9.2). Note that the sites follow a latitudinal order from north to south. Deposition data for the sites in Finland refer to 2017. Only genetic analyses were considered at these sites; thus, deposition data were not included in the main figures. NH_4^+ -N deposition in 2015 and 2016 for the site in Spain were not available due to problems with the measurements, so the averages for 2007–2014 are reported. Total nitrogen for the sites in Sweden, France and Spain is the sum of NH_4^+ -N and NO_3^- -N, because data for organic dissolved organic nitrogen were not available. Data for climate and deposition for Collelongo in Italy refer to long-term data and 2009, respectively^{67–69}

Country	Site	Species	N deposition level	Lat	Long	Altitude	Forest age	LAI	Soil type	T_a	P_a	NH_4^+	NO_3^-	TN			
				°N	°E	(m a.s.l.)	(y)	($\text{m}^2 \text{ m}^{-2}$)	(°C)	(mm)	(kg N $\text{ha}^{-1} \text{y}^{-1}$)						
											BD	TF	BD	TF	BD	TF	
Finland	Punkaharju ¹	PS	Low	61,77	29,33	98	90	n/a	Rustic Podzols	4.42	744	1.2	0.5	1.2	0.6	2.9	2.0
Finland	Kivalo ¹	PS	Low	66,36	26,73	73	65	n/a	Albic Arenosol	1.18	649	0.5	0.1	0.7	0.4	1.5	0.9
Finland	Sevetijarvi ¹	PS	Low	66,58	28,89	218	210	n/a	Rustic Podzols	-0.58	575	0.7	0.1	0.3	0.2	1.9	0.7
Sweden	Höka [#]	PS	Low	58,13	15,06	157	70	n/a	Podzols	6.8	532	2.0	0.5	1.4	1.1	3.4	1.5
UK	Thetford	PS	High	52,24	0,87	20	49	4.1	Arenosol	11.9	624	6.9	7	4.1	4.9	13	15
Belgium	Brasschaat	PS	High	51,30	4,51	14	87	1.8	Endogleyic Brunic Albic Hypoluvic Arenosol	10.6	855	7.5	12.1	5.6	7.7	15.8	25.4
UK	Rogate	PS	Low	51,10	-0,52	115	66	4.4	Podzols	11.7	747	4.4	5.8	2.9	3.5	9.7	13.1
UK	Alice Holt	FS	Low	51,15	-0,86	80	81	6.0	Gleysols	11.7	747	3.3	3.8	3.9	3.3	9	11.5
Belgium	Hoeilaart	FS	High	50,74	4,41	129	107	1.8	Albic Cutanic Alisol	10.4	787	6.1	8.2	6.2	7.2	15.7	22.1
France	Haguenauf [#]	PS	Low	48,85	7,71	175	91	2.1	Podzols	10.2	852	5.7	3.8	2.8	2.8	8.5	6.6
Switzerland	Schänis	FS	High	47,16	9,06	733	150	5.5	Eutric Cambisol	10.1	1951	7.5	7.6	5.3	5.5	14.7	17.8
Spain	Bertiz ^{2#}	FS	Low	43,16	-1,62	290	150	3.3	Leptic cutanic Alisol	12.9	1568	4.5	3.5	3.1	5.4	8.0	8.5
Italy	Collelongo ³	FS	Low	41,84	13,58	1560	125	5.5	Humic Acrisols	7.2	1140	3	3	3	5	7.5	12.7

¹ Deposition data at these sites refer to 2017. Only genetic analyses were considered at these sites, thus deposition data were not included in the main figures.

² NH_4^+ -N deposition in 2015 and 2016 were not available due to problems with the measurements, so the averages for 2007–2014 are reported.

[#]Total nitrogen is the sum of NH_4^+ -N and NO_3^- -N, because data for organic dissolved organic nitrogen were not available.

³ Source: [66, 67, 68]. Data for climate and deposition refer to long-term data and 2009, respectively.

Extended Data Table 2 | Differences between TF and BD for NH_4^+ , NO_3^- , and TN fluxes expressed as NH_4^+ -N, NO_3^- -N, and TN measured at each site. Differences are calculated from the annual deposition in 2016 and from long-term averages. We also report results from the two-sided t-test (for NO_3^- -N and TN) and the Wilcoxon-Mann-Whitney test (for NH_4^+ -N) for differences calculated for TF and BD fluxes in 2016. Diff indicates the difference between TF and BD for each form of nitrogen, and CI and df indicate the confidence interval and degrees of freedom, respectively. The sites follow a latitudinal order from north to south

Country	Site	TF-BD difference ($\text{kg N ha}^{-1} \text{y}^{-1}$)						Period
		2016		Long-term				
		NH_4^+	NO_3^-	TN	NH_4^+	NO_3^-	TN	
Sweden	Höka	-1.53	-0.3	-1.89	-1.79	-1.14	-2.93	1997-2018
UK	Thetford	0.1	0.8	2	3.2	2.2	7	1996-2016
Belgium	Brasschaat	4.6	2.1	9.6	9.6	3.6	15.5	1996-2016
UK	Rogate	1.4	0.6	3.4	-0.7	0	0.4	2010-2016
UK	Alice Holt	0.5	-0.6	2.5	0.6	0.3	3.9	2005-2010
Belgium	Hoeilaart	2.1	1	6.4	0.9	1	3	1996-2016
France	Haguenau	-1.87	-0.02	-1.89	2.31	2.17	4.49	1992-2016
Switzerland	Schänis	0.1	0.2	3.1	0.15	1.62	6	1999-2016
Spain	Bertiz	-1.36	1.92	0.56	-1.36	0.48	-0.69	2007-2016
Italy	Collelongo ¹	0	2	5.2	0	2	5.2	2009

Test	Nitrogen form	Hypothesis	Mean	CI	t	df	p value	
t-test	NO_3^- -N	Diff=0	0.77	0.07	1.47	2.4826	9	0.03
	TN	Diff=0	2.9	0.34	5.45	2.5631	9	0.03
			Median	CI	CI	W	df	p value
Wilcox. test	NH_4^+ -N	Diff=0	0.10	-1.53	-2.10	28	9	0.55

¹ We only had values for 2009.

Extended Data Table 3 | Concentrations of NO_3^- in the BD and TF water collected on different sampling dates. We also report $\delta^{15}\text{N}$ and $\delta^{18}\text{O}$ for each sampling date. n/a indicates that no values were measured for a sampling date due to very low NO_3^- concentrations and/or instrument failure. [1], [2] and [3] indicate the sampling dates detailed in the Supplementary Table 3

Site	Concentration (mg L^{-1})			$\delta^{15}\text{N}$ (‰)			$\delta^{18}\text{O}$ (‰)		
	BD		TF	BD		TF	BD		TF
	[1]; [2]; [3]	[1]; [2]; [3]	[1]; [2]; [3]	[1]; [2]; [3]	[1]; [2]; [3]	[1]; [2]; [3]	[1]; [2]; [3]	[1]; [2]; [3]	[1]; [2]; [3]
Höka	0.18; 0.34; 0.31	0.13; 0.42; 0.28	29.39; n/a; n/a	-1.17; n/a; 16.37	56.24		69.52; n/a; 64.86		
Thetford	0.48; 0.38; 0.5	1.31; 1.50; 1.79	-1.50; -7.48; -12.67	-2.62; -3.30; -19.19	33.59; 38.14; n/a		47.60; 42.74; 29.21		
Brasschaat	2.90; 1.66	5.85; 3.7	-24.91; -6.34	-8.99; 1.92	32.57; 35.36		39.38; 62.63		
Rogate	0.21; 0.29; 0.50	0.44; 0.52; 0.95	6.38; 1.99; 5.62	-2.17; -1.74; -0.88	61.06; 68.42; 65.12		46.05; 38.37; 54.51		
Alice Holt	0.45; 0.15; 0.49	0.47; 0.13; 0.40	6.36	9.75; -1.87; 5.41	63.85; n/a; n/a		40.24; 60.09; 50.17		
Hoeilaart	2.77; 2.28	4.70; 2.63	n/a; 14.68	-23.77; 6.54	n/a; 41.59		21.39; 16.19		
Haguenau ²	1.59; n/a; 1.42	4.69; n/a; 2.48	-4.17; -3.23; -7.29	21.39; n/a; 19.30	67.84; 71.75; 78.62		27.39; n/a; 34.05		
Schänis	1.03; 1.17; 0.37	1.46; 3.56; 0.31	14.74; 6.31; -6.95	0.77; -0.29; -2.04	66.61; 60.24; 67.64		67.27; 62.93; 21.45		
Bertiz ²	4.89; 1.33; 2.31	6.02; 1.70; 2.87	n/a; -6.85; 4.15	n/a; 11.05; 12.05	n/a; 47.93; 46.93		n/a; 10.32; 45.21		
Collelongo ³	0.64; 0.26; 0.29	0.66; 0.24; 0.30	6.21; 2.90; -6.21	-7.53; 11.06; 5.91	60.99; 66.20; 32.71		28.07; n/a; 55.89		

Extended Data Table 4 | $\Delta^{17}\text{O}$ values of NO_3^- in bulk deposition (BD) and throughfall (TF) for each sampling date (indicated as [1];[2];[3], see Supplementary Table 3) and the NO_3^- fraction derived from atmospheric and biological transformation (f_{Atm} and f_{Bio} , respectively) obtained using the mass-balance approach based on $\Delta^{17}\text{O-NO}_3^-$ in TF and BD (see Methods in the main text). Finally, we also show the partitioning between Biological and Atmospheric NO_3^- TF flux (mean and standard deviation, SD at each site), which was obtained by multiplying the total NO_3^- TF flux by f_{Bio} and f_{Atm} for each sampling date. n/a indicates that no values were measured for a sampling date due to very low NO_3^- concentrations and/or instrument failure. The data are shown in Figs. 2–4. Note that occasional values >1 and <0, for example Höka and the sampling dates for Thetford, Brasschaat, Haguenaau, Bertiz, and Collelongo (see Supplementary Text 1), were not included in the calculations of NO_3^- flux. Brasschaat* refers to isotopic measurements in NO_3^- obtained from wet-only collectors, in addition to the NO_3^- obtained from the traditional approach common at all sites and described in the Methods)

Site	$\Delta^{17}\text{O - NO}_3^- (\text{\textperthousand})$			NO_3^- fraction (f)			NO_3^- flux ($\text{kg N ha}^{-1} \text{y}^{-1}$)					
	BD			TF			Biological (f_{Bio})	Atmospheric (f_{Atm})	Biological	Mean (SD)	Atmospheric	Mean (SD)
	[1]; [2]; [3]	[1]; [2]; [3]	[1]; [2]; [3]	[1]; [2]; [3]	[1]; [2]; [3]	[1]; [2]; [3]	[1]; [2]; [3]	[1]; [2]; [3]	[1]; [2]; [3]	[1]; [2]; [3]	[1]; [2]; [3]	[1]; [2]; [3]
Höka	n/a; n/a; 17.21	28.19; 31.02; 23.77	<0	>1	-	-	-	-	-	-	-	-
Thetford	18.98; 18.93; 11.26	19.48; 23.41; 10.78	<0; <0; 0.04	>1; >1; 0.96	0.21	0.21	4.69	4.69	-	-	-	-
Brasschaat ⁽¹⁾	15.99; 16.68	7.18; 22.45	0.55; <0	0.45; >1	4.24	3.23 (1.79)	3.46	4.47 (1.79)	-	-	-	-
Brasschaat* ⁽¹⁾	16.14; 26.46	-	0.56; 0.15	0.44; 0.85	4.28; 1.17	-	3.42; 6.53	-	-	-	-	-
Rogate	24.12; 28.27; 27.66	19.24; 20.73; 21.91	0.20; 0.27; 0.21	0.80; 0.73; 0.79	0.71; 0.93; 0.73	0.79 (0.13)	2.79; 2.57;	2.71 (0.13)	2.77	-	-	-
Alice Holt ⁽²⁾	24.56; n/a; n/a	23.53; 25.58; 21.33	0.04; 0.10; 0.23	0.96; 0.90; 0.77	0.14; 0.31; 0.76	0.40 (0.32)	3.16; 2.99; 2.54	-	2.90 (0.32)	-	-	-
Hoeilaart	13.53; 15.50	2.70; 6.49	0.80; 0.58	0.20; 0.42	5.76; 4.18	4.97 (1.12)	1.44; 3.02	2.23 (1.12)	-	-	-	-
Haguenaau	23.63; 25.17; 34.84	20.92; 27.94; 28.18	0.11; <0; 0.19	0.89; >1; 0.81	0.32; 0.53	0.42 (0.15)	2.44; 2.23	2.34 (0.15)	-	-	-	-
Schänis	32.52; 29.61; 10.62	10.14; 8.30; n/a	0.69; 0.72; n/a	0.31; 0.28; n/a	3.79; 3.96	3.87 (0.12)	1.71; 1.54	1.63 (0.12)	-	-	-	-
Bertiz	n/a; 23.52; 11.55	n/a; 18.85; 15.70	0.20; <0	0.80; >1	1.07	1.07	4.30	4.30	-	-	-	-
Collelongo ⁽³⁾	31.53; 27.17; 7.98	n/a; n/a; 23.55	0.25; 0.13; 0	0.75; 0.87; >1	1.26; 0.67	0.97 (0.42)	3.74; 4.33	4.03 (0.42)	-	-	-	-

⁽¹⁾ To $\Delta^{17}\text{O}$ values measured in BD (Brasschaat) and wo (Brasschaat*) deposition correspond same $\Delta^{17}\text{O}$ values measured in TF.

⁽²⁾ In the mass balance approach we used $\Delta^{17}\text{O}$ values in BD measured in the nearby site Rogate (19 km apart).

⁽³⁾ Assuming the same values for $\Delta^{17}\text{O}$ TF in sampling dates [1] and [2].

Extended Data Table 5 | Results from the simple linear regression analyses for the relationships between f_{Bio} or gross canopy nitrification (GCN) and bulk deposition (BD) of total nitrogen (TN_{BD}) and of $\text{NH}_4^+ \text{-N}$ ($\text{NH}_4^+ \text{-N}_{\text{BD}}$). SE indicates standard error

Model	Estimate Slope (SE)	t-value	p-value	R^2
$f_{\text{Bio}} \sim \text{TN}_{\text{BD}}$	0.05 (0.01)	4.399	0.00039	0.53
$f_{\text{Bio}} \sim \text{NH}_4^+ \text{-N}_{\text{BD}}$	0.08 (0.03)	2.978	0.009	0.34
GCN ~ TN_{BD}	0.44 (0.08)	5.643	0.005	0.65
GCN ~ $\text{NH}_4^+ \text{-N}_{\text{BD}}$	0.65 (0.20)	3.268	0.000029	0.39